Available online at www.sciencedirect.com
SCIENCE DIRECT®
Journal of Power Sources 143 (2005) 142–149
JOURNAL OF POWER SOURCES
www.elsevier.com/locate/jpowsour

Novel anode structure for the direct methanol fuel cell☆

R.G. Allen, Chan Lim[1], L.X. Yang[2], K. Scott*, S. Roy

School of Chemical Engineering and Advanced Materials, University of Newcastle, Merz Court, Newcastle upon Tyne NE17RU, UK

Received 26 October 2004; accepted 26 November 2004
Available online 19 January 2005

Abstract

Pt–Ru catalysts have been made by a thermal decomposition and electrodeposition method onto a titanium mesh for the electrooxidation of methanol. Galvanostatic polarisations were used to assess and compare the relative activities of the electrodes. SEM and XRD are employed to study the morphology and structure of the catalyst layers. The performance of the anodes in fuel cell assemblies is also discussed. We can see that the mesh perform well in half and full cell tests despite significant apparent physical differences, which are yet to be explored.

Keywords: Methanol oxidation; Thermal decomposition; Electrodeposition; Fuel cell; Platinum; Ruthenium

1. Introduction

Solid polymer electrolyte direct methanol fuel cells are presently under active development. Based on a solid polymer electrolyte (SPE) in the form of a proton conducting membrane, direct methanol fuel cells (DMFCs) have the attraction of no liquid acidic or alkaline electrolyte and have shown improved performance in recent years particularly for applications in transport and various portable electronic devices [1]. Methanol is a liquid fuel that has substantial electroactivity and can be oxidised directly to carbon dioxide and water on catalytically active anodes in a DMFC.

At low temperature, liquid feed DMFCs are promising candidates for sources of portable and stationary power and in electric vehicular applications given the relatively simple system design and cell operation. However, obstacles such as low activity of methanol electrooxidation catalysts still prevent their widespread commercial applications [2,3]. Furthermore, carbon dioxide gas management is problematic and impedes further improvements to cell performance.

In operation, the DMFC oxidizes an aqueous solution of methanol forming carbon dioxide gas and protons. The carbon dioxide is then released into the anode structure:

$$CH_3OH + H_2O \rightarrow CO_2 + 6H^+ + 6e^- \quad (E_a = 0.02\,\text{V versus RHE}) \quad (1)$$

Protons generated at the anode pass through the solid polymer electrolyte membrane where they simultaneously combine with electrons and the oxidant (air or oxygen) reducing to water:

$$3/2O_2 + 6H^+ + 6e^- \rightarrow 3H_2O \quad (E_c = 1.23\,\text{V versus RHE}) \quad (2)$$

The overall cell reaction in a DMFC is the production of carbon dioxide and water as

$$CH_3OH + 3O_2 \rightarrow CO_2 + 2H_2O \quad (E_{cell} = 1.21\,\text{V}) \quad (3)$$

☆ This paper was presented at the 2004 Fuel Cell Seminar in San Antonio, TX, USA.

* Corresponding author. Tel.: +44 191 2228700; fax: +44 191 2225292.
E-mail addresses: chanlim@dymos.co.kr (C. Lim), lianxi.yang@nrc.gc.ca (L.X. Yang), k.scott@ncl.ac.uk (K. Scott).
[1] Present address: Dymos, Inc., Frontier Technology Research Team, Hyundai Automotive Group, Seoul, Republic of Korea. Tel.: +82 31 728 1480; fax: +82 31 728 1411.
[2] Present address: Shape Transfer Processes, Integrated Manufacturing Technologies Institute, Room 240-1, 800 Collip Circle, London, Ont., Canada N6G 4X8. Tel.: +1 519 430 7133; fax: +1 519 430 7064.

0378-7753/$ – see front matter © 2004 Elsevier B.V. All rights reserved.
doi:10.1016/j.jpowsour.2004.11.038

The typical structure of the DMFC anodes used in the DMFC is essentially successive layers of supported/unsupported catalyst bonded with Nafion resin, Teflon-bonded carbon black diffusion layer (GDL), and a carbon cloth or paper diffusion layer. This structure is far from suitable for the transport and release of carbon dioxide gas from the anode, resulting potentially in considerably high hydrodynamic and mass transport limitations for methanol at the anode. As a result, a gradual deterioration in electrical performance can occur.

We have shown in previous work at Newcastle [3] that the removal of carbon dioxide produced can be improved by using stainless steel mesh at the anode. While the results showed promising behaviour in terms of gas removal characteristics and electrical performance, the standard carbon supported MEA construction was still used in the work. Based on these results, recent efforts have been made to utilise mesh with the electrocatalysts deposited directly onto the surface.

The use of titanium metal substrates, either plate or large aperture mesh, is common in the electrochemical industry. There are many documented catalyst synthesis methods, including chemical reduction, colloids, electrodeposition, sol–gel and thermal decomposition [4]. The chlor-alkli industry makes extensive use of a thin catalyst layer prepared on titanium mesh by thermal decomposition. The technique, producing highly promising properties of the oxides of platinum group metals, was disclosed by Beer [5] in the early 1960s, and is presently known as the route to produce dimensionally stable anodes (DSAs).

This publication will report the progress of integrating into fuel cells the Pt–Ru catalyst layers prepared via two routes: thermal decomposition and electrodeposition. Electrochemical characterisation of such electrodes for the oxidation of methanol has been carried out and is reported. This is a continuation in our research to develop titanium mini-mesh catalytic electrodes which can be directly hot pressed onto a solid polymer electrolyte membrane and used in a fuel cell [6,7,9,11].

2. Experimental details

2.1. Mesh catalyst layer preparation

Catalyst coatings on the titanium mesh were prepared using thermal decomposition and electrodeposition. Before applying the catalyst layer the titanium mesh was first etched in boiling hydrochloric acid (35%) for about 30 s to remove the well-adhered surface oxide layers. This etching process also provides a rough surface onto which the electrocatalyst can be more securely anchored [8]. This was followed by a thorough distilled water rinse. The preparation methods used for thermal decomposition and electrodeposition have been described elsewhere [9,10]. In summary, for thermal decomposition the mesh was dipped multiple times into a precursor solution (e.g. 0.2 M $H_2PtCl_6{\cdot}6H_2O$ in ethanol + 0.2 M $RuCl_3{\cdot}xH_2O$ in isopropanol) until the desired loading was achieved. The final decomposition was performed in air at 430 °C for 1 h. The electrodes fabricated in this way are designated Pt–RuO_2/Ti (Pt:Ru = 1:1 in atomic ratio). For electrodeposition, the mesh was placed in a divided cell in a 0.004 M $H_2PtCl_6{\cdot}6H_2O$ + 0.004 $RuCl_3{\cdot}xH_2O$/1 M H_2SO_4 plating solution. The counter electrode used during the deposition was a 25 mm × 25 mm platinum mesh and deposition was carried out at a polarised current of 4 mA cm^{-2} for 1 h.

2.2. Anode electrochemical measurements

Electrochemical measurements were performed using a Gill AC potentiostat (ACM Instruments), controlled with ACM Sequencing Software, version 5. All experiments were conducted in a N_2-deaerated, three-electrode cell. The working electrodes were lacquered (Miccroshield, Hi-Tek Products Ltd.), leaving a window of 1 cm^2 exposed. The counter electrode was a platinum mesh measuring 25 mm × 25 mm and the reference electrode was a mercury sulphate (MMS) (Hg/Hg_2SO_4/0.5 M (0.680 V, RHE). Unless otherwise specified, electrode potentials are referenced against the reversible hydrogen electrode (RHE). The electrolyte solution used in the electrochemical characterisation was of 0.5 M H_2SO_4/x M CH_3OH solution, which was prepared with reagent grade chemicals and deionised water.

It was observed that the electrochemical behaviour of the newly prepared anode changes in its early life, due to so-called “hydration” or “wetting effects”, or a maturation process [11]. The anodes were therefore conditioned by immersing and cycling between 0 and 900 mV in 0.5 M H_2SO_4 until a stable state of the electrode was reached. The electrochemical measurements were then carried out. Potential-time transients were recorded at constant current densities (galvanostatic polarisation). The anode potential was allowed to stabilize for up to 3 min before collecting data.

2.3. Fuel cell assembly

In this study, fuel cells were assembled using the standard Newcastle small-scale DMFC flow bed design and manifold arrangement [12]. A simple schematic of the fuel cell assembly can be seen in Fig. 1.

The cathode in the membrane electrode assembly (MEA) was constructed by first forming the gas diffusion layer (GDL). An appropriate amount of Ketjenblack (EC 300J) and 15 wt.% Teflon (33%, Fluon) was dispersed in isopropanol

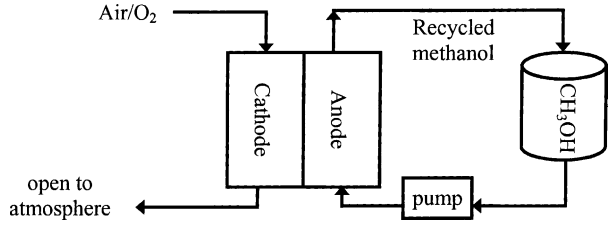

Fig. 1. Fuel cell system schematic.

and ultrasonicated until evenly dispersed. A spray gun (Model 100 LG, Badger) was then used to evenly distribute the dispersion onto a commercial 20 wt.% wet-proofed carbon paper (Toray 090, E-Tek) to form a ca. 1 mg cm^{-2} GDL. The ink for the cathode catalyst layer was made by dispersing supported platinum (60 wt.% Pt/C XC72, E-Tek) with an appropriate amount of Nafion solution (5 wt.%, EW: 1100 Aldrich) to make a 1 mg Pt cm^{-2} catalyst layer with 15 wt.% Nafion. This ink was then sprayed on top of the GDL. Prior to fuel cell assembly, a 1 mg cm^{-2} layer of Nafion diluted with isopropanol was sprayed on top of the catalyst layer and allowed to dry in air.

The conventional anode was fabricated in a similar manner to the cathode, although the GDL was not utilised. The ink for the anode catalyst layer was made by dispersing supported platinum–ruthenium (60 wt.% Pt–Ru/C XC72, 1:1 at.% E-Tek) with an appropriate amount of Nafion solution (5 wt.%, EW: 1100 Aldrich) to make a 1 mg Pt–Ru cm^{-2} catalyst layer with 15 wt.% Nafion. This ink was then sprayed on top of the GDL. Prior to fuel cell assembly, a 1 mg cm^{-2} layer of Nafion diluted with isopropanol was sprayed on top of the catalyst layer and allowed to dry in air.

The mesh anodes were fabricated as discussed above, although for fuel cell testing the mesh was dipped into the dilute Nafion solution and dried, achieving a loading of 0.8–1 mg cm^{-2} to aid electronic activity.

Each MEA was composed of a pre-treated Nafion 117 membrane (EW 1100, Dupont), the cathode as prepared above, and the desired anode. The loading of the catalyst layer on the mesh anodes used in the fuel cell was ca. 1 mg cm^{-2} (1:1 at.% Pt:Ru). The MEA was then hot-pressed at 125 °C and 50 kg cm^{-2} for 3 min, cooled and then placed into the single cell 9 cm^2 active area for galvanostatic investigation. The cell was composed of two high-density graphite blocks, impregnated with phenolic resin, into which parallel gas/liquid flow channels (width and depth 1 mm) are machined. The ridges between the channels provide electrical contact to the MEA. Flexible electrical heaters (Watson Marlow) were mounted at the rear of the graphite blocks to maintain the desired cell temperature, which was controlled through a temperature controller and monitored by a thermocouple positioned inside one of the two graphite blocks. Electrical contact was made using gold-plated metallic bolts screwed into the blocks. During operation, a 1.0 M solution of aqueous methanol was fed to the anode at a rate of ca. 12 cm^3 min^{-1}. Unheated and non-humidified air was supplied to the cathode at a flow rate of 1.0 mL min^{-1}, without back pressure. For anode polarisations, H_2 was supplied to the cathode side.

2.4. Physical analysis

X-ray diffraction data for the anode catalyst powder and electrode were obtained using Philips Xpert Pro diffractometer operating at 40 kV accelerating voltage and 40 mA of beam current, and using Cu $K\alpha_1$ radiation. Analysis of the XRD data was carried out using Philips Xpert High Score. Diffraction peaks were attributed following the Joint Committee of Powder Diffraction Standards (JCPDS) cards. The selected 2θ range was from 20° to 70° scanning at a step of 0.03°. The surface and cross-sectional morphologies of the anode catalyst layers were surveyed by a Jeol 6300 scanning electron microscope (SEM), equipped with computerized digital image software.

3. Results and discussion

3.1. Morphological observation

SEM was employed to view the differences in the morphology and structure of the two types of mesh catalyst coatings. Shown in Fig. 2 are the images of the Pt–Ru catalyst layers prepared by electrodeposition, and in Fig. 3 images of the layers prepared by thermal decomposition. The thermal decomposed coatings have been discussed in more detail in a previous publication [6,7,9,11].

On a macroscopic level (Figs. 2a and 3a), both coating types exhibit a rough surface which should allow increased access of methanol to the catalyst, leading to enhanced catalytic activity. The thermal coating can be seen to have dried between the mesh strands and covers the mesh openings. It contains numerous cracks which were likely formed during the decomposition of chlorine compounds and evaporation of water. The electrodeposited catalyst layer sticks more closely to the mesh strands and is quite rough in morphology, due to the porosity induced by gas evolution while electroplating.

At higher magnification, the electrodeposited layer can be seen (Fig. 2b and c) to be an agglomeration of submicron-sized particles. EDX analysis suggests that the coating is homogeneous in composition, being a Pt–Ru mixture of approximately 60% Pt and 40% Ru. The thermal coating shows variation in coating morphology and EDX reveals inhomogeneity in its composition. As shown in Fig. 3b and c, the microstructure is composed of a cracked thin film region of nano-sized particles with micron-sized particles on top of the film and submicron-sized particles underneath the film. The resolution of the SEM machine is not sufficient to further investigate the finer structure. EDX analysis shows that the film is mainly composed of Pt and Ru whereas the particles on top of the film are Ru and oxide rich. It seems likely that the Ru atoms inside the thin film diffuse out during the thermal treatment, forming RuO_2 particles on top of the thin film.

3.1.1. X-ray diffraction analysis (XRD)

XRD analysis was collected to help further characterise the coatings and highlight areas of similarity and difference between thermally decomposed, electrodeposited and conventional catalyst layers (Fig. 4). Shown in Fig. 5 is the X-ray diffraction data for the plain mesh, a typical thermal

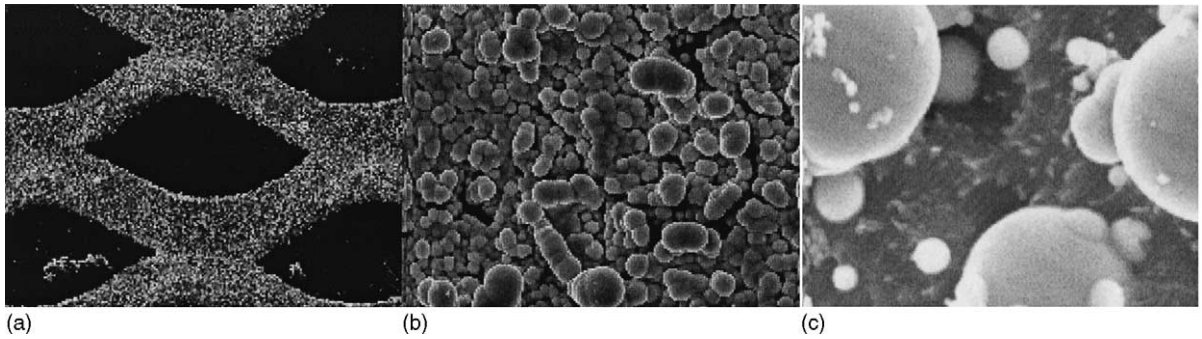

Fig. 2. (a–c) SEM images of the Pt–Ru catalysts as electrodeposited on Ti mesh support.

and electroplated coated mesh, and Etek 60% Pt–Ru (1:1) catalyst powder. Typical peaks of the crystalline face centred cubic (fcc) Pt(1 1 1), (2 0 0), (2 2 0), (3 1 1), and (2 2 2) planes as well as the Ti substrate are clearly visible. The diffraction peak at 25° is the (0 0 2) plane of the hexagonal structure of the Vulcan XC-72 carbon support of the commercial catalyst. The mean particle size of the agglomerates was evaluated from the line broadening of the (2 2 0) peak using the Scherrer formula. It was estimated to be about 5 nm for both the electroplated and the thermally decomposed mesh coatings. This is larger than commonly reported for powder catalysts (Etek = 2 nm). The presence of oxide peaks, likely corresponding to RuO_2 (JCPDS-ICC#40-1290) appears only on the thermally decomposed samples. Using the 28.2° the oxide size was estimated to be about 34 nm.

If one compares the position of the Pt(2 2 0) and (3 1 1) peaks on the two mesh coatings (Fig. 6) a clear difference between the locations of the peaks is evident. From Vegards law, it is assumed that peak position shifts to higher angles (i.e. lower lattice parameter) of this nature correlates to the formation of a solid solution of Pt–Ru as the Pt lattice con-

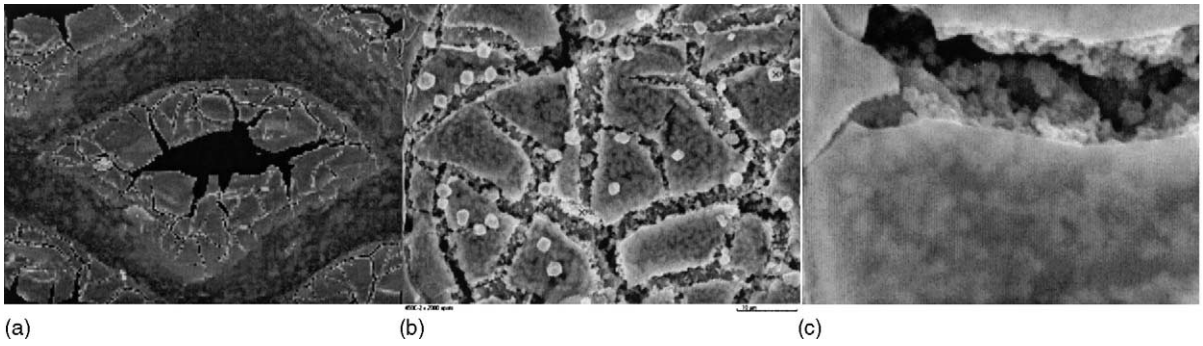

Fig. 3. (a–c) SEM images of the Pt–Ru catalysts as thermally decomposed on Ti mesh support.

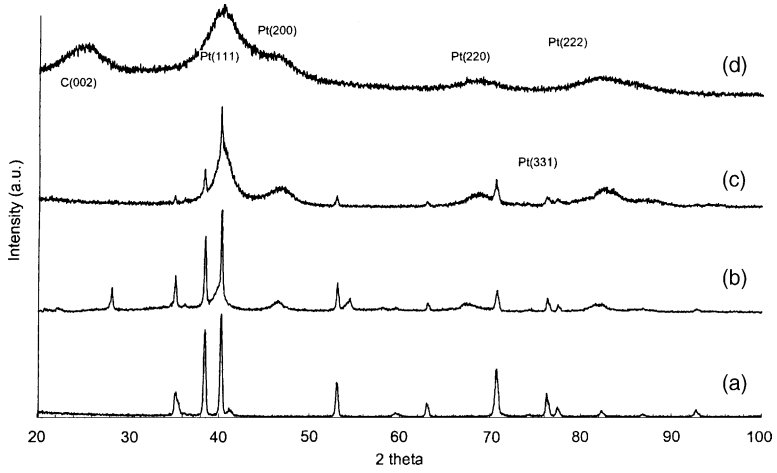

Fig. 4. XRD: (a) Ti base; (b) thermally decomposed; (c) electrodeposited; (d) Etek 60% Pt–Ru/C (1:1 at.%).

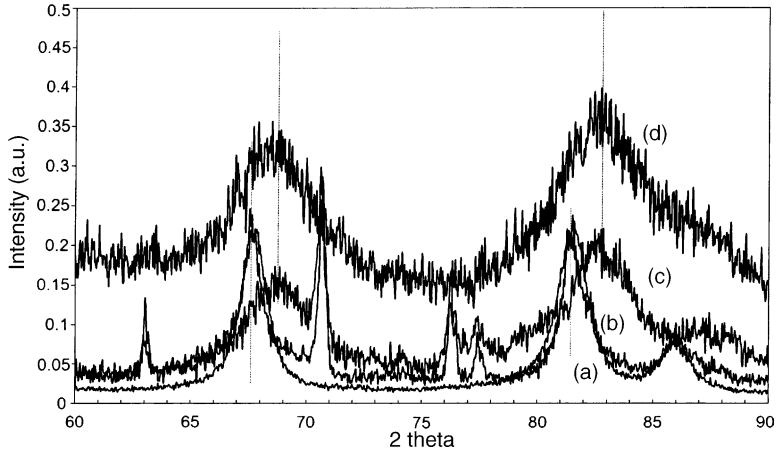

Fig. 5. Close up XRD: (a) Pt black; (b) thermally decomposed; (c) electrodeposited; (d) Pt–Ru black (1:1 at.%).

tracts due to the replacement of some Pt atoms by the smaller Ru atoms (rRu = 0.133 nm and rPt = 0.138 nm [13]).The peak positions of the thermal decomposed coincide directly with those of Pt black. This indicates no alloying of Ru to the Pt in the layer. Comparing the electrodeposited peak positions to that of unsupported Pt–Ru (Johnson Matthey), we see good correlation. This suggests a similar degree of Pt–Ru alloying. Lattice parameters can be evaluated from the angular position

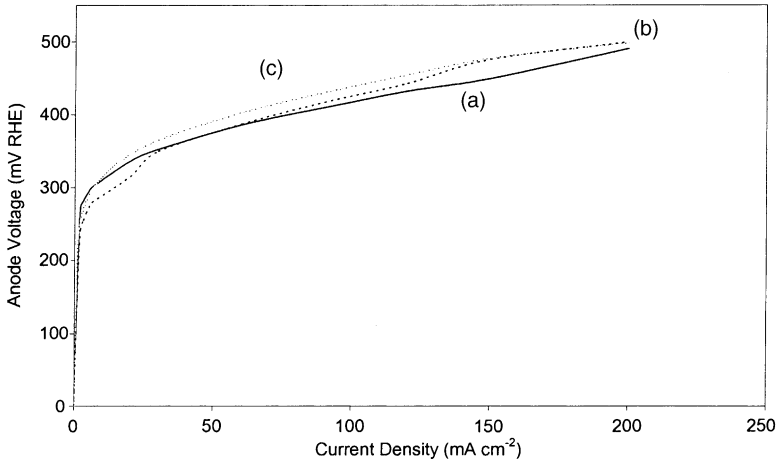

Fig. 6. Galvanostatic performance in 2 M CH_3OH/0.5 M H_2SO_4 (60 °C) for: (a) conventional anode; (b) thermally decomposed; (c) electrodeposited on Ti support.

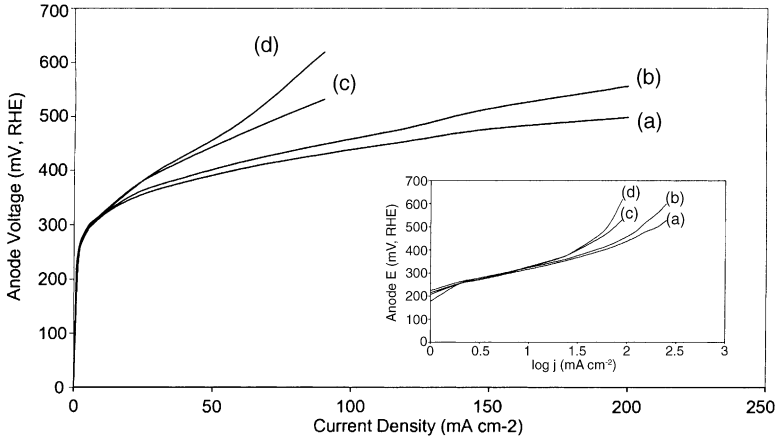

Fig. 7. Methanol oxidation in *x* M CH_3OH/0.5 M H_2SO_4: (a) 2 M; (b) 1 M; (c) 0.5 M; (d) 0.2 M. The inset shows the logarithmic plots of current densities vs. electrode potential at (a) 2, (b) 1, (c) 0.5 and (d) 0.2 M.

of the peak maxima:

$$a_{\mathrm{fcc}} = \frac{\lambda_{k\alpha 1}}{2} \frac{\sqrt{h^2 + k^2 + l^2}}{\sin \theta_{\max}} \quad (4)$$

yielding an average of 0.3865 nm for the electrodeposited samples and 0.3909 nm for the thermal decomposed samples. Using the relationship provided in literature between lattice parameters and atomic pt fractions [14] this suggests compositions as shown in Table 1. It can be seen that they differ from those obtained by EDX, although these values should be taken with a note of caution, as the authors [15,16] have estimated a degree of error of 0.5% in their correlation. However, the difference does support the conclusion that the composition of the thermal decomposed coating is inhomogeneous in nature, likely due to the mixed oxides on the surface. XPS analysis will help to clarify the coating composition and will be reported in future publications.

3.2. Methanol oxidation

3.2.1. Comparison of mesh-supported to conventional catalysts

Galvanostatic measurements were carried out from 0.0 to 200 mA cm^{-2}, to further compare their electrochemical performance and are shown in Fig. 6. After polarising there was an initial transient, possible due to the establishment of adsorption equilibrium. At higher currents (say, above 200 mA cm^{-2}) slow potential increases were observed. This is due to catalyst poisoning by the formation of stable adsorbent species such as carbon oxides.

It can be seen that there is virtually no difference between the three anode types under the test conditions used. This is surprising, given the porosity of the conventional catalyst compared to the mesh-supported catalysts. It is expected that future research will investigate the mesh coatings further in an effort to explain the mesh activity despite comparatively lower porosity.

3.2.2. Comparison between mesh coating types

To explore the effect of methanol concentration on the mesh anodes, galvanostatic polarisations with *x* M CH_3OH/0.5 M CH_3OH at various temperatures is shown in Fig. 7. The inset shows the logarithmic plots of current densities versus electrode potential at (a) 2, (b) 1, (c) 0.5 and (d) 0.2 M. The inset shows the logarithmic plots of current densities versus electrode potential at the same concentrations.

To explore the effect of temperature on the anodes, the galvanostatic polarisations with 2 M CH_3OH/0.5 M CH_3OH at (a) 25, (b) 60 and (c) 90 °C is shown in Fig. 8. The inset shows the logarithmic plots of current densities versus electrode potential at the same temperatures. In both the cases, the thermal decomposed and the electroplated anodes display the same characteristics. The improvement between 25 and 60 °C is marked, with a slight increase in performance when the temperature is further elevated to 90 °C. A similar large increase in performance can be seen from 0.2 to 0.5 M methanol concentration.

Estimations of the Tafel slopes obtained from the Tafel plots in the insets of Figs. 7 and 8 are displayed in Table 2. The variation of the slope at 60 °C at 1 and 2 M indicates that the methanol oxidation mechanism is modified by temperature as commonly reported. All observed values fall into typical range of 90–120 mV dec^{-1} for the methanol oxidation reaction [16,17].

Table 1
Coating composition in at.%

Coating type	EDX		XRD	
	Pt	Ru	Pt	Ru
Thermally decomposed	48	52	85	15
Electrodeposited	66	34	51	49

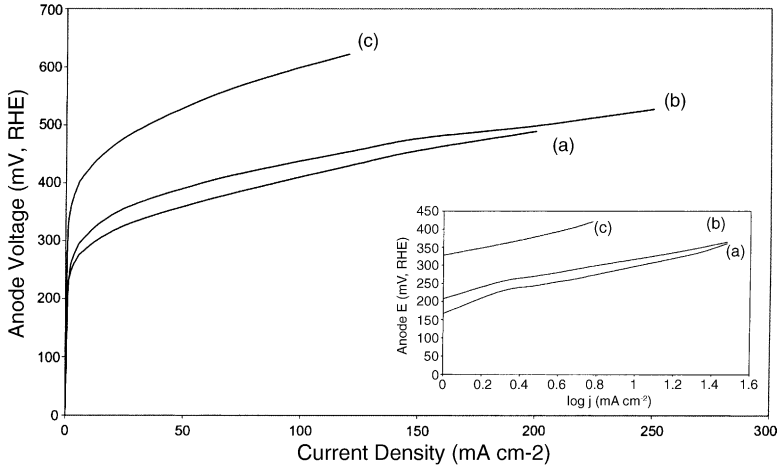

Fig. 8. Methanol oxidation in 2 M CH_3OH/0.5 M H_2SO_4: (a) 90 °C; (b) 60 °C; (c) 25 °C. The inset shows the logarithmic plots of current densities vs. electrode potential at (a) 90, (b) 60 and (c) 25 °C.

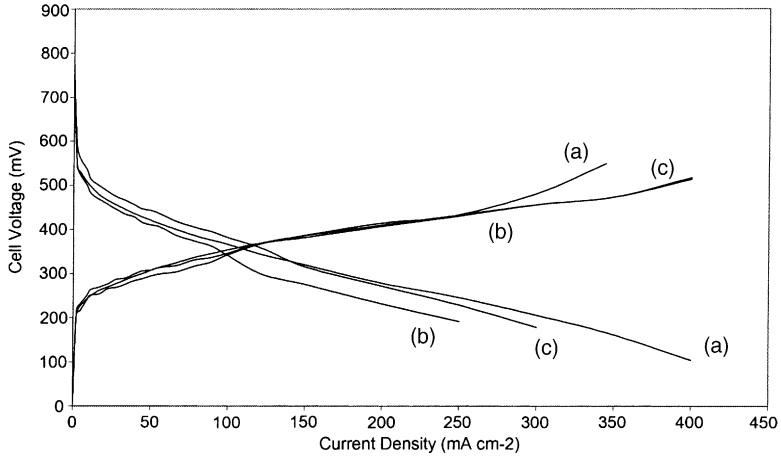

Fig. 9. Fuel cell polarisation of MEA using various anodes measured at 90 °C in 1 M CH_3OH; cathode catalyst layer: 1 mg cm^{-2} 60 wt.% Pt/C; electroplated anode catalyst layer 1 mg cm^{-2}. Air feed, 0 bar back pressure. The anodes are (a) conventional anode, (b) thermally decomposed and (c) electrodeposited on Ti support.

Table 2
Tafel slopes for mesh electrodes

CH_3OH conc. (M)	T (°C)	Tafel slope
	25	118
2	60	100
	90	120
0.2		118
0.5		118
1	60	100
2		100

3.3. Fuel cell

Fig. 9 shows the preliminary direct methanol fuel cell (DMFC) results of mesh-based anodes compared to the conventional structure. Consistent with half cell polarisations shown in Fig. 6, it can be seen that the mesh coatings formed by thermal decomposition (b) and electrodeposition (c) display comparable performance to each other and conventional anodes (a). Additionally, MEAs operating with a mesh anode compare favourably with recently published DMFC work [18,19] under comparable operating conditions. For example, at 225 mA cm^{-2}, the cell voltage reported in Ref. [18] is approximately 210 mV and the power density is about 600 mW cm^{-2} while that of the mesh MEA is 310 mV and the power density is 700 mV cm^{-2}. The increased cell operating temperature and, most frequently pressure, in other reported work, such as [19] make numerical comparison difficult.

In the reported mesh MEAs, the DMFC anode is sandwiched directly between the graphite flow channels and the Nafion membrane of the MEA. This design appears to allow effective gas release from the catalyst surface with little detrimental effect on the fuel cell overpotential. Although from XRD analysis the thermal decomposed catalyst layer has larger particle size and less Ru content than the commercial Pt–Ru black, the mesh-based anode performed well because its open structure allows gaseous carbon dioxide to diffuse out easily from the catalyst layer and hence retains high catalyst utilisation during cell operation.

This concept defines the strategy of our laboratory in searching for new anodes for the DMFC. The new anode possesses a superior methanol activity to the carbon powder supported catalysts used previously [2] and further work will allow comparison of the conventional, thermally decomposed, and electrodeposited anodes to be made. Overall, our results indicate that significant increases in the catalytic activity for methanol oxidation may be achieved in the future by optimisation of both the mesh anode and the overall MEA construction.

4. Conclusions

This work has discussed the use of fabricated Pt-based electrocatalysts deposited on titanium mesh by thermal decomposition and electrodeposition of metal salt precursors. The electrodes were successfully used for the oxidation of methanol in acidic methanol electrolytes and preliminary results suggest that the catalysed titanium mesh is a promising alternative candidate to carbon-supported catalysts for methanol oxidation. Further investigation of the mesh coatings is required as the differences between the structures created using thermal decomposition and electrodeposition need to be understood to further explain catalytic activity and physical differences.

Future publications will report progress in a number of important areas related to this project. To further compare the two coating methods the effect of methanol concentration and temperature on the polarisation behaviour has been studied by electrochemical impedance spectroscopy (EIS). Additionally, XPS analysis of the mesh coatings is ongoing. To help to characterise the mesh in fuel cell situations, fuel cell flow visualizations and detailed fuel cell parametric studies will be conducted.

Overall, our results indicate that increases in the catalytic activity for methanol oxidation may be achieved in the future by optimization of both the mesh anode and the overall MEA construction.

Acknowledgements

EPSRC supported R.G. Allen, L.X. Yang and Chan Lim in this work. The MOD supported the work through the joint grant scheme no. JGS/826. The work was performed in research facilities provided through an EPSRC/HEFCE Joint Infrastructure Fund award no. JIF4NESCEQ. Mesh was supplied by DEXMET Corporation, USA. The advice of C.L. Jackson and G.A. Rimbu was gratefully received during the fuel cell work in this project.

References

[1] A.S. Aricò, S. Srinivasan, V. Antonucci, DMFCs: from fundamental aspects to technology development, Fuel Cells 1 (2) (2001) 133–161.
[2] K. Scott, W.M. Taama, P. Argyropoulos, Engineering aspects of the direct methanol fuel cell system, J. Power Sources 9 (1) (1999) 43–59.
[3] K. Scott, P. Argyropoulos, P. Yiannopoulos, W.M. Taama, Electrochemical and gas evolution characteristics of direct methanol fuel cells with stainless steel mesh flow beds, J. Appl. Electrochem. 31 (8) (2001) 823–832.
[4] Y. Takasu, Y. Murakami, Design of oxide electrodes with large surface area, Electrochim. Acta 45 (25–26) (2000) 4135–4141.
[5] H.B. Beer, The invention and industrial development of metal anodes, J. Electrochem. Soc. 127 (8) (1980) 303c–307c.
[6] L.X. Yang, R.G. Allen, K. Scott, P. Christensen, S. Roy, A new Pt–Ru anode formed by thermal decomposition for the DMFC, J. Fuel Cell Sci. Technol., 2005, in press.
[7] L.X. Yang, R.G. Allen, K. Scott, P. Christensen, S. Roy, A study of Pt–RuO_2 catalysts thermally formed on titanium mesh for methanol oxidation, Electrochim. Acta 5 (2004) 1217–1223.
[8] E.H. Yu, K. Scott, Direct methanol alkaline fuel cell with catalysed metal mesh anodes, J. Electrochem. Commun. 6 (4) (2004) 361–365.
[9] Lim, Chan, K. Scott, R.G. Allen, S. Roy, Direct methanol fuel cells using thermally catalysed Ti mesh, J. Appl. Electrochem. 34 (9) (2004) 929–933.
[10] R.G. Allen, Ph.D. Thesis, University of Newcastle upon Tyne, 2005.
[11] L.X. Yang, R.G. Allen, K. Scott, P. Christensen, S. Roy, A comparative study of Pt–Ru and Pt–RuSn thermally formed on Ti support for methanol electrooxidation, J. Power Sources 137 (2) (2004) 257–263.
[12] P. Argyropoulos, K. Scott, A.K. Shukla, C. Jackson, A semi-empirical model of the direct methanol fuel cell performance. Part I. Model development and verification, J. Power Sources 123 (2) (2003) 190–199.
[13] J.A. Dean (Ed.), Lange's Handbook of Chemistry, 13th ed., McGraw-Hill, New York, 1985, pp. 3-124–3-125.
[14] H.A. Gasteiger, N. Markovic, P.N. Ross Jr., E.J. Cairns, Methanol electrooxidation on well-characterized Pt–Ru Alloys, J. Phys. Chem. 97 (46) (1993) 12020–12029.
[15] V. Ramilovic, H.A. Gasteiger, P.N. Ross Jr., Structure and chemical composition of a supported Pt–Ru elecrocatalyst for methanol oxidation, J. Catal. 154 (1) (1995) 98–106.
[16] P.A. Christensen, A. Hamnett, G.L. Troughton, The role of morphology in the methanol electro-oxidation reaction, J. Electroanal. Chem. 362 (1–2) (1993) 207–218.
[17] A.S. Arico, Z. Poltarzewski, H. Kim, A. Morana, N. Giordano, V. Antonucci, Investigation of a carbon-supported quaternary Pt–Ru–Sn–W catalyst for direct methanol fuel cells, J. Power Sources 55 (2) (1995) 159–166.
[18] A.K. Shukla, C.L. Jackson, K. Scott, G. Murgia, A solid-polymer electrolyte direct methanol fuel cell with a mixed reactant and air anode, J. Power Sources 111 (1) (2002) 43–51.
[19] X. Ren, P. Zelenay, S. Thomas, J. Davey, S. Gottesfeld, Recent advances in direct methanol fuel cells at Los Alamos National Laboratory, J. Power Sources 86 (1–2) (2000) 111–116.